ORIGINAL RESEARCH

miR-15a/15b Cluster Modulates Survival of Mesenchymal Stem Cells to Improve Its Therapeutic Efficacy of Myocardial Infarction

Yingfeng Tu, MD, PhD; Yan Qiu, MD; Li Liu, MD, PhD; Tao Huang, MD, PhD; Hao Tang, MD; Youbin Liu, MD, PhD; Wenguang Guo, PhD; Hongchi Jiang, MD; Yuhua Fan, PhD; Bo Yu, MD, PhD

***Background*—**The poor viability of transplanted mesenchymal stem cells (MSCs) hampers their therapeutic efficacy for ischemic heart disease. MicroRNAs are involved in regulation of MSC survival and function. The present study was designed to investigate the molecular effects of miR-15a/15b on MSC survival, focusing on the role of vascular endothelial growth factor receptor 2.

***Methods and Results*—**We first harvested donor luc(Luciferase)-MSCs (5×10^5) isolated from the luciferase transgenic mice with FVB background. Luc-MSCs were transfected with miR-15a/15b mimics or inhibitors and cultured under oxygen glucose deprivation condition for 12 hours to mimics the harsh microenvironment in infarcted heart; they were subjected to MTT (3-(4,5-dimethyl-2-thiazolyl)-2,5-diphenyl-2-H-tetrazolium bromide Thiazolyl Blue Tetrazolium Bromide) assay, bioluminescence imaging, quantitative reverse transcription–polymerase chain reaction, transferase-mediated deoxyuridine triphosphate–digoxigenin nick-end labeling assay, and flow cytometry. Furthermore, the levels of vascular endothelial growth factor receptor 2, protein kinase B, p(Phosphorylate)-protein kinase B, Bcl-2, Bax, and caspase-3 proteins were available by Western blotting assay. In vivo, acute myocardial infarction was induced in 24 mice by coronary ligation, with subsequent receipt of Luc-MSCs, Luc-MSCs+miR-15a/15b inhibitors, or PBS treatment. The therapeutic procedure and treatment effects were tracked and assessed using bioluminescence imaging and echocardiographic measurement. Next, ex vivo imaging and immunohistochemistry were conducted to verify the distribution of MSCs. We demonstrated that miR-15a/15b targeted vascular endothelial growth factor receptor 2 to modulate MSC survival, possibly via phosphatidylinositol 3-kinase/protein kinase B signaling pathway, which was proved by bioluminescence imaging, immunohistochemistry analysis, and echocardiographic measurement.

***Conclusions*—**Luc-MSCs could be followed dynamically in vitro and in vivo by bioluminescence imaging, and the role of miR-15a/b could be inferred from the loss of signals from luc-MSCs. This finding may have practical clinical implications in miR-15a/15b–modified MSC transplantation in treating myocardial infarction. **(*J Am Heart Assoc*. 2019;8:e010157. DOI: 10.1161/JAHA.118.010157)**

Key Words: cardiac • cardiac contractility and energetics • cardiac development • cardiac dysfunction

Ischemic heart disease is the leading cause of death worldwide.[1,2] Severe ischemic heart disease, especially myocardial infarction (MI)–mediated heart failure, causes a significant loss of functional cardiomyocytes. However, the heart is an organ with limited self-renewal ability because adult cardiomyocytes can hardly regenerate in vivo. Over the past decades, several lines of experimental research and clinical trials have documented beneficial roles of stem cell transplantation to improve heart function after MI, which remains a promising approach for the treatment of coronary artery disease, MI, and heart failure.[3,4] Mesenchymal stem cells (MSCs), with advantages in multilineage and in potential

From the Department of Cardiology, The 2nd Hospital of Harbin Medical University, Nangang District, Harbin, China (Y.T., H.T., Y.L., B.Y.); The Key Laboratory of Myocardial Ischemia, Chinese Ministry of Education, Harbin, Heilongjiang, China (Y.T., Y.L., B.Y.); Department of Geriatrics, Huadong sanatorium, Wuxi City, Jiangsu Province, China (Y.Q); Department of Anesthesiology, The Third Hospital of Harbin Medical University, Harbin, Heilongjiang, China (L.L.); Department of Radiology, The Fourth Hospital of Harbin Medical University, Harbin, China (T.H.); College of Pharmacy (Y.F.) and College of Basic Medical Science (W.G.), Harbin Medical University–Daqing, Daqing, China; and Key Laboratory of Hepatosplenic Surgery, Department of General Surgery, The First Affiliated Hospital of Harbin Medical University, Harbin, China (H.J.).

Correspondence to: Bo Yu, MD, PhD, Department of Cardiology, The Second Hospital of Harbin Medical University, The Key Laboratory of Myocardial Ischemia, Chinese Ministry of Education, Harbin 150008, China. E-mail: yubodr@163.com and Yuhua Fan, PhD, Harbin Medical University–Daqing, Harbin-Daqing, Heilongjiang 163319, China. E-mail: fyh198306@126.com

Received June 21, 2018; accepted November 29, 2018.

Clinical Perspective

What Is New?

- This study demonstrates that knockdown of miR-15a/15b has beneficial effects on mesenchymal stem cells (MSCs) by promoting proliferation, inhibiting apoptosis, increasing vascular endothelial growth factor receptor 2 expression, and improving their survival within the myocardial infarction zone.
- In addition, the beneficial effects of miR-15a/15b are possibly a result of activation of the vascular endothelial growth factor receptor 2/phosphatidylinositol 3-kinase/protein kinase B signaling pathway.
- Furthermore, bioluminescence imaging strategy provides a unique and powerful method to monitor the biological activity of MSCs in vitro and in vivo, which will be extremely valuable in the diagnosis and treatment application of clinical patients in the future.

What Are the Clinical Implications?

- These findings suggest the potential for miR-15a/15b to be an alternative therapeutic target to improve MSC survival in vitro and in vivo.
- Regulating microRNA expression in stem cells is likely to emerge as an alternative and safe method to treat ischemic heart disease.
- Low survival rate after transplantation in heart tissue is one of the crucial limitations accounting for the hampered cardiac repair role of MSCs.
- The potential to prevent MSC apoptosis and death to improve ischemic heart function and decrease mortality is highly clinically relevant.

immunologic privilege, and easy to be acquired, have been widely studied in both clinical trials and animal models.[5–7] And the previous research has suggested that MSC transplantation exerts therapeutic effect on ischemic heart disease.[8] However, low survival rate after transplantation in heart tissue is one of the crucial limitations accounting for the hampered cardiac repair role of MSCs.[9] Many studies have confirmed that the harsh microenvironment with ischemia, oxidative stress, inflammation, and mechanical stress contributes to the great cell apoptosis and death.[10,11] Optimizing the approaches to augment engrafted cell survival and improve its function is a prerequisite to translate this therapeutic strategy into clinics. Hence, various strategies have been used in attempt to overcome this obstacle, and many of them have showed promising results.

MicroRNAs are short 20- to 22-nucleotide RNA molecules that are expressed in a tissue-specific and developmentally regulated manner.[12] Recently, many microRNAs are expressed and considered to be important regulators in cardiac development and pathophysiological features.[13] In addition, recent studies indicate a novel strategy for enhancing the efficacy of human MSCs using microRNAs is on the upsurge.[14,15] Seo et al demonstrated that injection of miR-146a–transfected human MSCs after cardiac ischemia/reperfusion injury led to a reduction of fibrosis area and increased vascular endothelial growth factor (VEGF) expression, confirming the regenerative capacity, such as reparative angiogenesis in the infarcted area.[16] Lee et al disclosed injected miR-133a promoted human MSCs differentiated into cardiac-like cells through targeting epidermal growth factor receptor.[17] Functional annotation of the predicted targets for miR-15a, miR-15b, miR-16, miR-195, miR-424, and miR-497 suggests that these microRNAs control a complex network of genes involved in cell cycle, proliferation, apoptosis, and survival.[18,19] Liu et al have disclosed that miR-16 enhances differentiation of human MSCs in a cardiac niche toward myogenic phenotypes in vitro.[20] To date, the role of miR-15a/15b cluster in regulating MSC survival and function under hypoxia condition has not been fully disclosed. In the current study, we identified the VEGF receptor 2 (VEGFR-2) gene among the targets of miR-15a and miR-15b, which was downregulated in MSCs under oxygen and glucose deprivation (OGD) condition. Moreover, the role of miR-15a/15b in regulating MSC survival rate after transplantation into MI zone has never been explored before. Therefore, determining the role of miR-15a/15b in MSC biology and function and its molecular mechanisms could be of major significance for stem cell–based therapy aimed at regeneration of heart tissue.

Conventional methods to monitor stem cell transplantation are inconvenient and time-consuming and cannot be repeated. These methods usually require us to kill an animal and visualize stem cells by using immunohistochemical staining of stem cell–specific markers. Therefore, there is a strong impetus for developing novel imaging approaches that would allow noninvasive assessment of myocardial response to cell therapy in vivo. Recently, bioluminescence imaging (BLI) has contributed to detecting stem cell survival conveniently and continuously, for this imaging technique can provide a noninvasive and efficient observation of stem cell growth in vitro and in vivo. In this current study, we used in vitro and in vivo BLI to noninvasively track the fate of luc-MSCs isolated from the luciferase transgenic mice with FVB background, which are stably transduced with firefly luciferase reporter gene.

In short, the aims of the present study are to demonstrate that miR-15a/15b may play a significant role in regulating survival of MSCs and in improving engraftment after transplantation. And we put forward that blockade of specific miR-15a/15b cluster in MSCs can modulate their survival and effects in vitro and in vivo.

Materials and Methods

Animals

Eight-week-old male FVB/N mice were supplied by the Beijing Vital River Laboratory Animal Technology Co, Ltd and the luciferase transgenic FVB/N mice were purchased from Xenogen Corporation. Mice were fed under standard animal room conditions (humidity, 55%–60%; temperature, 25°C). Food and water were freely available throughout the experiments. All experimental protocols were preapproved by the Experimental Animal Ethic Committee of Harbin Medical University (Animal Experimental Ethical Inspection Protocol No. 2009104).

Isolation and Culture of MSCs

Bone marrow MSCs were isolated from the luciferase transgenic FVB mice (25–28 g), as previously described.[21] In brief, total luc-MSCs were flushed with culture medium from the femur and tibia and seeded in MSC basal medium (StemCell Technologies, Vancouver, BC, Canada, http://www.stemcell.com) supplemented with MSC stimulatory supplements (StemCell Technologies) and penicillin (100 U/mL)/streptomycin (100 U/mL) in culture flasks at 37°C in 5% CO_2, 95% air in a humidified incubator. The first medium change was performed to remove the nonadherent cells at 48 hours. When grown to 90% confluence, cells were harvested with 0.25% trypsin (Sigma) and passaged at a ratio of 1:3. All the cells used in this study were then harvested when reaching 80% confluence by 0.25% trypsin (Sigma) at passage 3.

Transfection of miR-15a/15b inhibitors or Mimics Into Cultured MSCs

The cells were seeded in antibiotic-free medium for 24 hours before transfection. For the miR-15a/15b knockdown, the cells were transfected with miR-15a/15b inhibitors (GenePharma Co Ltd) using Lipofectamine 2000 (Invitrogen). Transfection complexes were added to medium at final oligonucleotide concentration of 50 nmol/L. The culture medium was replaced 4 hours after transfection with the regular culture medium for another 24 hours. MicroRNA transfection efficiency was proved by quantitative reverse transcription–polymerase chain reaction (qRT-PCR). For the miR-15a/15b upregulation, the cells were transfected with miR-15a/15b mimics (GenePharma Co Ltd) using Lipofectamine 2000.

Oxygen and Glucose Deprivation

On the day of the experiment, the culture medium was removed, the cells were washed with warm Phosphate Buffered Saline (PBS), and then the experimental medium was added. For experiments, the experiment medium was MSC basal medium and the cells were kept at normal culture conditions (21% oxygen and with glucose). To achieve OGD, a technique was used similar to that described before.[22] Briefly, the OGD experimental medium (MSC basal medium without glucose) was gassed with nitrogen for 30 minutes and then added to cell culture wells, which had been washed 3 times with PBS. OGD was induced by incubating cells in a humidified airtight chamber (Billups-Rothberg Inc, Del Mar, CA) equipped with an air lock and continuously flushed with 95% N_2/5% CO_2 for 15 minutes under 37°C. The airtight chamber was then sealed and kept in a 37°C incubator for 4, 8, 12, or 24 hours. The oxygen concentration was <0.2%, as monitored by an oxygen analyzer (Sable Systems, Las Vegas, NV).

Dual-Luciferase Reporter Assay

The region of the VEGFR-2 3′-untranslated region (UTR) containing the potential binding site of miR-15a/b was predicted using TargetScan, version 7.1. The sequence was inserted into the 3′ region of the luciferase gene in a luciferase vector (wt-Luc-VEGFR-2; Shanghai GeneChem Co, Ltd, Shanghai, China), and a mutated version of this sequence was inserted into the vector (mu-Luc-VEGFR-2). HEK 293T cells (Guangzhou Liang Zi Kang Biotechnology, Guangzhou, China) were plated at 2×10^5 cells per well in 24-well plates. The following day, cells were cotransfected with 80 ng of pMIR-REPORT Luciferase vector, including the 3′-UTR of VEGFR-2 (with either wild-type or mutant miR-15a/15b binding sites), pRL-TK control vector (encoding Renilla luciferase, 8 ng), and miR-15a/15b mimics or mimics control at a final concentration of 50 nm by using Lipofectamine 2000 (Invitrogen), according to the manufacturer's instructions. In addition, we further demonstrated that miR-15a/15b may inhibit Bcl-2 expression through direct interaction with predicted binding sites located in the 3′-UTR region of Bcl-2; we also cloned a reporter vector in which luciferase cDNA was followed by a fragment of the 3′-UTR from Bcl-2 mRNA containing the putative miR-15a or miR-15b binding sequences. And we synthesized another luciferase reporter fused to the Bcl-2 3′-UTRs, but with a mutant miR-15a or miR-15b binding sequence. The pRL-TK vector (Promega Corporation) expressing Renilla luciferase served as a control. Twenty-four hours after transfection, dual-luciferase assays were performed using the Dual-Glo Luciferase Assay System (Promega). Normalized data were calculated as the quotient of Renilla/firefly luciferase activities. Each experiment was repeated for at least 3 times in each group.

MTT Test

Primary culture luc-MSCs were plated in 96-well plates and treated with OGD (4, 8, 12, and 24 hours). After the treatment period, the serum-free medium was removed, and then the cells were cultured

with regular culture medium for another 48 hours. To further disclose the role of miR-15a/15b on the MSC survival, luc-MSCs were plated in 96-well plates and treated with OGD 12 hours, OGD 12 hours+miR-15a inhibitors, OGD 12 hours+miR-15b inhibitors, OGD 12 hours+miR-15a mimics, OGD+miR-15b mimics, or OGD 12 hours+miR-15a/15b inhibitors. To monitor cell survival, MSCs were incubated for 4 hours with 0.5 mg/mL of MTT (Sigma) and resuspended in 150 μL of dimethyl sulfoxide (Sigma). Absorbance was recorded at 490 nm using an Easy Reader 340 AT (SLT-Lab Instruments). Results are presented as percentage of survival, taking the control as 100% survival.

In Vitro Bioluminescent Assays of Luc-MSC Survival

The luciferase signals of the luc-MSCs from different treatment were monitored using BLI at 0, 4, 8, 12, and 24 hours after OGD treatment. When imaging firefly luciferase gene (Fluc) of luc-MSCs in the well, the cultured cells were treated with D-luciferin (150 μg/mL final concentration) and Fluc images were acquired 5 minutes later. The images for Fluc activity were measured using an IVIS 100 imager (Xenogen, Alameda, CA) and an exposure time of 10 seconds. Peak bioluminescence signals were expressed as photons per square centimeter per second per steradian (photons/s/cm^2/sr), which was measured using Living Image software 3.2 (Xenogen).

Transferase-Mediated Deoxyuridine Triphosphate–Digoxigenin Nick-End Labeling Analysis

Apoptosis-induced DNA fragmentation was determined using the transferase-mediated deoxyuridine triphosphate–digoxigenin nick-end labeling (TUNEL) assay. The luc-MSCs from different groups were fixed with 4% (w/v) paraformaldehyde and processed by using a commercial kit (Roche) in accordance with the manufacturer's instructions. TUNEL staining was done using the in situ cell death detection kit (Roche), and the nuclei were stained with 4′,6-diamidino-2-phenylindole for 10 minutes. The data were expressed as a percentage of the area of TUNEL-positive cells in 10 random fields. The luc-MSC apoptosis was determined by Image Pro Plus software.

Cell Apoptosis Analysis by Fluorescence-Activated Cell Sorting

We used OGD to induce luc-MSC apoptosis. In brief, after cells were washed with PBS, the culture medium was replaced with serum-free MSC basal medium without glucose. Fluorescence-activated cell sorting analysis was performed as previously described. Cell apoptosis was determined using an annexin V–fluorescein isothiocyanate apoptosis detection kit (BD Biosciences). Briefly, 2.0×10^5 cells were resuspended in 0.5 mL of binding buffer and incubated with annexin V–fluorescein isothiocyanate and propidium iodide for 10 minutes in the dark at room temperature. A fluorescence-activated cell sorting flow cytometer (BD Biosciences) equipped with a fluorescein isothiocyanate signal detector FL1 (excitation, 488 nm, green) and a phycoerythrin emission signal detector FL3 (excitation, 585 nm, red) was used to analyze cellular apoptosis. We performed 3 independent tests. The results were calculated using the Cell Quest Pro software (BD Biosciences) and expressed as the percentage of apoptotic cells of the total cells.

Cardiac Infarction Animal Models

FVB/N mice were anesthetized with pentobarbital sodium (50 mg/kg, IP) before endotracheal intubation. After anesthesia, the animals were placed in a supine position and surface leads were placed subcutaneously to record an electrocardiogram. All surgical procedures were performed under aseptic conditions. A lateral thoracotomy (1.5-cm incision between the third and fourth ribs) was performed to provide exposure of the left anterior descending coronary artery. MI was produced via the ligation of left coronary artery, as previously described. Sham-operated control mice underwent the same procedures, except that the suture placed under the left coronary artery was not tied. Ischemia was confirmed by visual observation (cyanosis) and by observing ST-segment elevation and QRS widen on echocardiography.

Implantation of MSCs

Twenty-four FVB/N mice were used for construction of the ischemic model. Seven days after the ligation, the 24-model MI FVB/N mice were equally randomized to 1 of 3 groups: (1) the MSC group, in which luc-MSCs in suspension were injected intramuscularly at the left anterior free wall using an insulin syringe with a 30-gauge needle; (2) the miR-15a/15b inhibitors–MSC group, in which the animals were injected intramuscularly luc-MSC+miR-15a/15b inhibitors suspension; and (3) the PBS group, in which the animals were injected with PBS. Cell implantation was performed 1 week after induction of acute MI. PBS or cell solutions were injected at 6 injection sites into anterior and lateral aspects of the viable myocardium bordering the infarction (total 5.0×10^6 cells in 0.1 mL). After injection, the chest was closed and the animals were allowed to recover.

BLI of Luc-MSC Transplantation

The bioluminescence signals of the luc-MSCs were monitored using BLI at 1, 7, 14, 21, and 28 days after implantation. Five

mice in each group were anesthetized with 2.5% (v/v) isoflurane and transferred into the chamber of an in vivo optical imaging platform (Bruker In-Vivo Multispectral FX PRO). To acquire images of Fluc, the mice were directly injected intraperitoneally with 150 mg/kg body weight of D-luciferin. Ten minutes later, the bioluminescence signals of luc-MSCs were acquired with 1 minute of exposure time. Peak bioluminescence signals were expressed as photons/s/cm^2/sr, as described before,[23] which was measured using living image software (Bruker MI). For ex vivo cardiac imaging, hearts were explanted and immediately immersed in 5-mm culture dishes containing 2 to 3 mL of 12 mol/L D-luciferin in PBS. Images were acquired using a 1- to 2-minute interval until peak signal was observed.

Tissue Fixation and Immunohistochemical Analysis

After intubation, the chest was opened and the heart was perfusion fixed for 2 minutes at 120 mm Hg with 4% paraformaldehyde (Sigma-Aldrich, St Louis, MO; http://www.sigma-aldrich.com) in PBS via left ventricular stab (a right atrial defect provided the egress for blood and fluid). Fixed hearts were immersed in 30% sucrose overnight, embedded into optimal cutting temperature compound (Sakura Finetek, Torrence, CA; http://www.sakuraeu.com), frozen, and prepared into 10-μm-thick frozen sections. In brief, slides were blocked by 5% donkey serum in 1% BSA for 20 minutes and incubated with the goat anti-luciferase antibody (1:300; Santa Cruz Biotechnology, Inc, Santa Cruz, CA), and rabbit polyclonal anti–α-actinin (Santa Cruz Biotechnology Inc) staining was performed. Slides were washed with PBS 3 times, incubated with the donkey anti-goat Alexa Fluor 488 (1:1000; Invitrogen) and the rat anti-rabbit Alexa Fluor 555 (1:1000; Invitrogen) for 60 minutes at room temperature in dark, and washed and mounted. Confocal microscopy was performed on a Leica SP5 confocal system (Leica, Wetzlar, Germany).

Quantitative Reverse Transcription–Polymerase Chain Reaction

Total RNA samples from cultured MSCs were isolated using Trizol reagent (Invitrogen), according to manufacturer's protocols. Total RNA (0.5 μg) was then reverse transcribed using High-Capacity cDNA Reverse Transcription Kit (Applied Biosystems) to obtain cDNA. The SYBR Green PCR Master Mix Kit (Applied Biosystems) was used to quantify the RNA levels of miR-15a and miR-15b, with U6 as an internal control. The VEGFR-2 and Bcl-2 in MSCs were detected also using qRT-PCR analysis, with GAPDH as an internal control. The primers for mouse miR-15a/b were designed as follows: miR-15a forward, 5′-TAGCAGCACATAATGG-3′; miR-15a reverse, 5′-GTGCAGGGTCCGAGGT-3′; miR-15b forward, 5′-ATGAACTT TCTCTGTCTTGG-3′; miR-15b reverse, 5′-TCACCGCCTCGGCT TGTCACA-3′; U6 forward, 5′-CTCGCTTCGGCAGCACA-3′; and U6 reverse, 5′-AACGCTTCACGAATTTGCGT-3′. The primers for VEGFR2, Bcl-2, and GAPDH were designed as follows: VEGFR-2 forward, 5′-GGCTAACGTGTCCTGCCAG-3′; VEGFR-2 reverse, 5′-AGTACCAACGCACAGTGATATTG-3′; Bcl-2 forward, 5′-GTCGCTACCGTCGTGACTTC-3′; Bcl-2 reverse, 5′-CAGACATG-CACCTACCCAGC-3′; GAPDH forward, 5′-TGGATTTGGACGCA TTGGTC-3′; and GAPDH reverse, 5′-TTTGCACTGGTACGTGTTG AT-3′. The qRT-PCR was performed on 7500 FAST Real-Time PCR System (Applied Biosystems) for 40 cycles.

Echocardiography

Five weeks after acute MI treatment, mice from different treatment groups were anesthetized with 2.5% (v/v) isoflurane and placed on the experimental platform. Transthoracic echocardiography was performed using a high-resolution in vivo ultrasound imaging system with a 40-MHz phased array transducer (Panoview β1500; Cold Spring Biotech Corp, Taiwan). Two-dimensional guided M-mode tracings were recorded from the parasternal long-axis view at the midpapillary muscle level. When the picture was stabilized, left ventricular end-diastolic dimensions, left ventricular end-systolic dimensions, left ventricular fractional shortening, and left ventricular ejection fraction were measured. All measurements were made from >3 beats and averaged. After functional measurement, mice were euthanized and hearts were collected in 4% paraformaldehyde or liquid nitrogen for use.

Masson Trichrome Staining

The left ventricle was fixed in 4% paraformaldehyde for 48 hours and embedded with paraffin. Cross-sectional slices along the minor axis were obtained with a microtome. Masson trichrome staining (Sigma-Aldrich, HT15-1KT) was used to evaluate collagen deposition, according to the manufacturer's instructions. Sections were imaged at ×200 magnification by bright-field microscopy (IX71; Olympus, Japan).

Western Blot Analysis

Briefly, the protein concentrations were determined with a bicinchoninic acid protein assay kit using bovine serum albumin (BSA) as the standard. Equal amounts of protein (60 μg) were fractionated by SDS-PAGE and blotted to polyvinylidene difluoride membrane (Millipore, Bedford, MA). Membranes were blocked for 1 hour using 5% nonfat milk in Tris-buffered saline with Tween. Then, they were probed overnight at 4°C with the following primary antibodies:

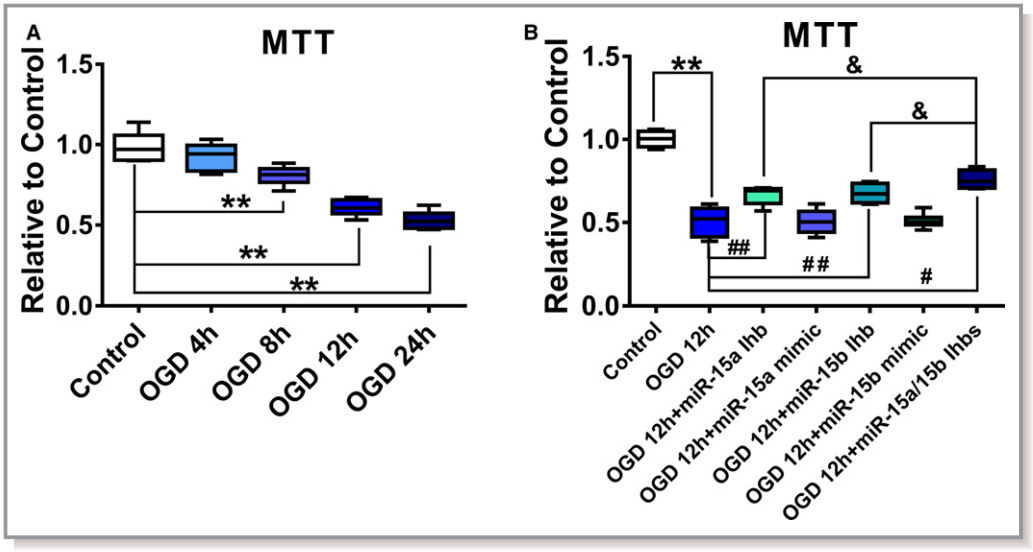

Figure 1. The effect of oxygen and glucose deprivation (OGD) on the proliferation of luc-mesenchymal stem cells (MSCs) in vitro. **A**, luc-MSCs were treated with OGD for 4, 8, 12, or 24 hours. Cell viability was detected by MTT assays. Data are expressed as median (quartile 1–quartile 3), n=6. $^{*}P<0.05$, $^{**}P<0.01$ vs Control. **B**, luc-MSCs were pretreated with miR-15a/15b inhibitors or miR-15a/15b mimics for 24 hours and then cultured under OGD condition for 12 hours. Cell viability was also detected by MTT assays. Data are expressed as median (quartile 1–quartile 3), n=6. $^{**}P<0.01$ vs Control; $^{\#}P<0.05$, $^{\#\#}P<0.01$ vs OGD group; $^{\&}P<0.05$ vs OGD plus miR-15a/15b inhibitors treated group.

VEGFR-2 (1:1000 dilution; Cell Signaling Technology), phosphatidylinositol 3-kinase (PI3K; 1:500 dilution; Cell Signaling Technology), p-PI3K (1:500 dilution; Cell Signaling Technology), protein kinase B (AKT; 1:1000 dilution; Cell Signaling Technology), p-AKT (1:1000 dilution; Cell Signaling Technology), Bcl-2 (1:500 dilution; Abcam), Bax (1:200 dilution; Abcam), caspase-3, and anti-GADPH (1:5000 dilution; Cell Signaling), all in 5% milk in Tris-buffered saline with Tween. After incubation with the primary antibodies, membranes were incubated with secondary antibody (1:8000 dilution; Alexa Fluor 700 goat anti-mouse IgG [H+L] or Alexa Fluor 800 goat anti-rabbit IgG [H+L]; Invitrogen) in PBS at room temperature for 1 hour. Western blot bands were captured by using the Odyssey Infrared Imaging System (LI-COR Biosciences, Lincoln, NE) and quantified with Odyssey v1.2 software (LI-COR Biosciences) by measuring the band intensity (area×OD (optical density)) in each group and normalizing to GAPDH as an internal control. Unless otherwise stated, Western blot experiments were repeated 3 times.

Statistical Analysis

All quantitative data were expressed as median (quartile 1–quartile 3) and analyzed by SPSS 13.0 software. Wilcoxon rank sum and Kruskal-Wallis tests were used for statistical evaluation of the data. Differences were considered as statistically significant when $P<0.05$.

Results

OGD-Induced Damage in Luc-MSCs

To mimics the harsh microenvironment in infarcted heart, the luc-MSCs were cultured in a humidified airtight chamber equipped with an air lock and continuously flushed with 95% N_2/5% CO_2 for 15 minutes under 37°C. The airtight chamber was then sealed and kept in a 37°C incubator for 4, 8, 12, and 24 hours. Along with the increase of the OGD treatment time, the luc-MSC viability determined by MTT analysis was gradually decreased with prolongation of OGD treatment time, which was reduced nearly by 35% in cells on OGD for 12 hours relative to no OGD treatment (Figure 1A).

Knockdown of miR-15a/15b Expression Reduces OGD-Induced Damage in Luc-MSCs

Next, we investigated the possible cytoprotective effect of miR-15a/15b on OGD-induced damage in luc-MSCs. The cells were transfected with miR-15a mimics, miR-15a inhibitors, or miR-15b mimics or inhibitors for 12 hours and then cultured under OGD condition for 12 hours. The MTT results indicated that pretreatment with miR-15a or 15b inhibitors reduced OGD-induced luc-MSC apoptosis, while not with miR-15a or miR-15b mimics pretreatment (Figure 1B). Moreover, the cytoprotective effect of miR-15a/15b inhibitors cocktail on OGD-induced damage in luc-MSCs was more effective than miR-15a or miR-15b inhibitors separately. The above data

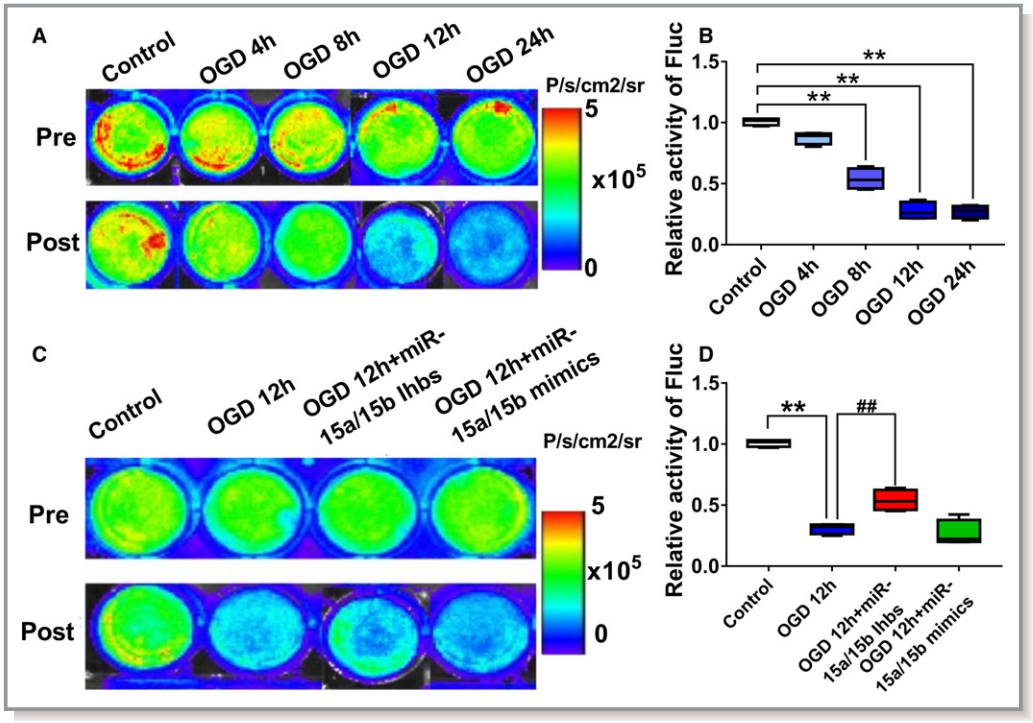

Figure 2. In vitro visualization and region of interest (ROI) analysis of firefly luciferase gene (Fluc) activities to monitor the mesenchymal stem cells under oxygen and glucose deprivation (OGD) condition. **A** and **B**, Quantitative signals from imaging in vitro were obtained by ROI analysis and were shown next to each well picture. The bioluminescence imaging (BLI) results showed a drastic decrease in Fluc activities with prolongation of OGD treatment time, especially in the OGD 12 hour and OGD 24 hour groups. Data are expressed as median (quartile 1–quartile 3), n=6 independent experiments for each condition. $^{**}P<0.01$ vs Control. **C** and **D**, Quantitative signals from Control, OGD 12 hours, OGD 12 hour+miR-15a/15b inhibitors, and OGD 12 hour+miR-15a/15b mimics groups imaging in vitro were obtained by ROI analysis and were shown next to each well picture. The BLI results showed a drastic decrease in Fluc activities in the OGD group after 12 hours OGD stimulation relative to Control, but the miR-15a/15b inhibitors treatment could partially reverse the decrease induced by OGD. Data are expressed as median (quartile 1–quartile 3), n=6 independent experiments for each condition. $^{**}P<0.01$ vs Control; $^{\#\#}P<0.01$ vs OGD 12 hour group.

manifested that knockdown of miR-15a/15b expression in luc-MSCs substantially attenuated OGD-induced damage in luc-MSCs in vitro.

In Vitro Visualization of Luc-MSC Survival Under OGD Condition Controlled by miR-15a/15b

To detect the luc-MSC survival under OGD condition repetitively and in real-time, we transfected miR-15a/15b mimics or inhibitors into MSCs cultured under the OGD condition, and then we detected the luc-MSC survival via a serial of BLI analysis in vitro. The results of the BLI analysis in vitro from this study showed that, compared with no OGD stimulation, the Fluc activity of luc-MSCs decreased gradually with prolongation of OGD stimulation, especially at 12 and 24 hours OGD treatment (Figure 2A and 2B). When normalized to results from pretreatment, the percentage bioluminescence signals from miR-15a/15b inhibitors treatment group demonstrated a significant reverse relative to OGD treatment group, indicating luc-MSC survival could be improved via miR-15a/15b inhibitor treatment, not miR-15a/15b mimics treatment, under the OGD 12 hour condition (Figure 2C and 2D).

VEGFR-2 and Bcl-2 Are the Target Genes of miR-15a/15b

One of the predicted targets of miR-15a/15b is VEGFR-2 by using the specific program TargetScan (http://www.targetscan.org) (Figure 3A). As shown in Figure 3, the miR-15a/15b mimics administered at a concentration of 50 nmol/L decreases luciferase activity of the reporter vector containing miR-15a/15b binding sequences (Figure 3C and 3E). However, the miR-15a/15b mimics has no significant effect on the reporter vector with mutated miR-15a/15b binding sequences (Figure 3D and 3F). These data suggest that miR-15a/15b may inhibit translation of VEGFR-2 by directly acting on response elements specific for miR-15a/15b in the VEGFR-2 3′-UTR region. In addition, another predicted target of miR-15a/15b is

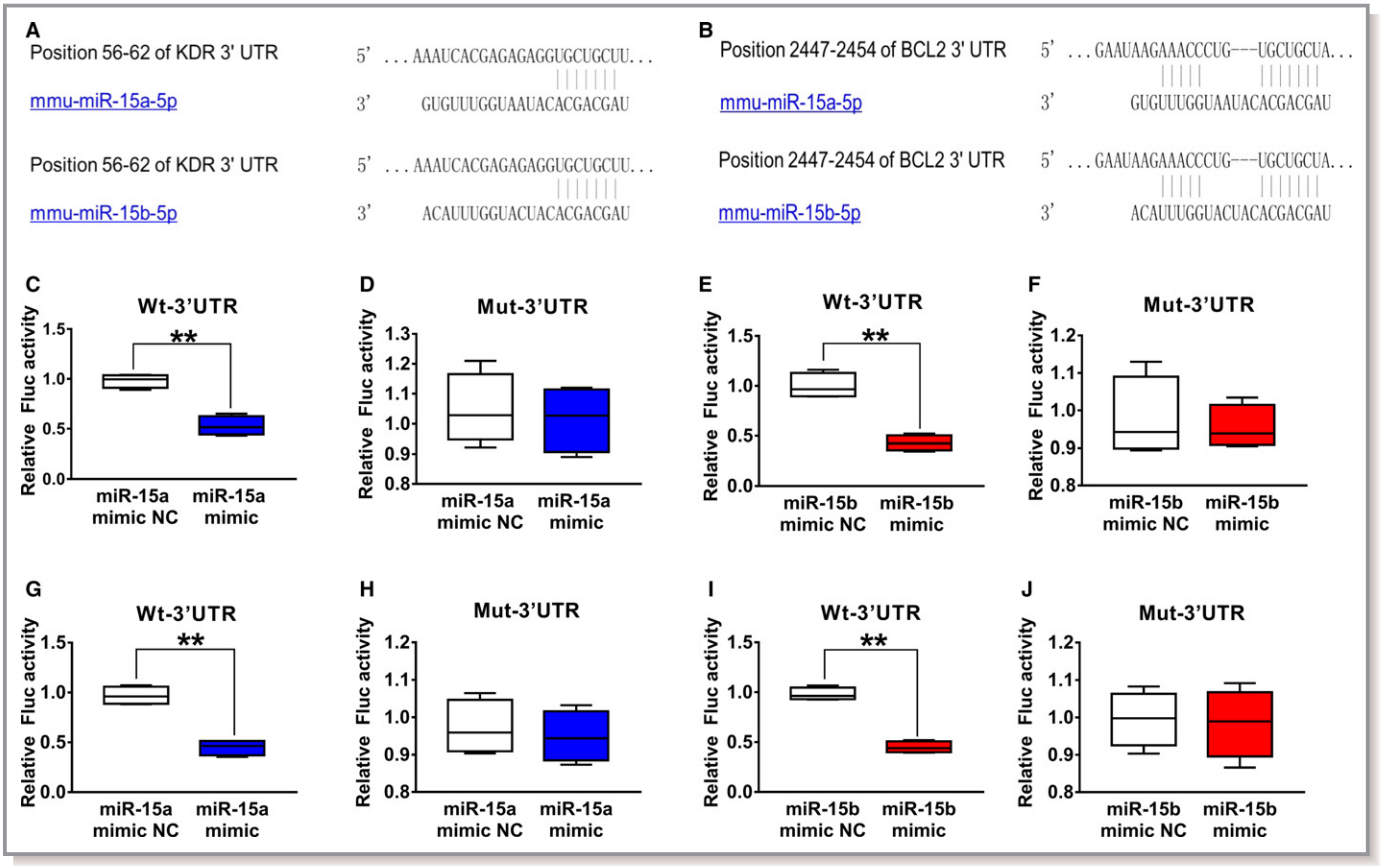

Figure 3. Vascular endothelial growth factor receptor 2 (VEGFR-2) and Bcl-2 were validated as a target of miR-15a/15b. **A**, The 3′-untranslated region (UTR) of VEGFR-2 harbored a potential targeting site of miR-15a/15b, which was conserved among mouse by bioinformatics analysis. **C** and **E**, Luciferase assay was performed to show that overexpression of miR-15a/15b in HEK 293T cells could significantly suppress the luciferase activity of a reporter fused with 3′-UTR of VEGFR2 mRNA. HEK 293T cells were transfected with a pMIR-VEGFR2-3′-UTR or pMIR-VEGFR2-m3′-UTR. Meanwhile, the cells were cotransfected with an miR-15a/15b mimics or mimics negative control (NC). Compared with the mimics NC, the miR-15a/15b mimics could reduce luciferase activity containing a wild-type miR-15a/15b binding site (**C** and **E**) but not a mutant binding site (**D** and **F**). **B**, 3′-UTR of Bcl-2 harbored a potential targeting site of miR-15a/15b, which was conserved among mouse by bioinformatics analysis. **G** and **I**, Luciferase assay was performed to show that overexpression of miR-15a/15b in HEK 293T cells could significantly suppress the luciferase activity of a reporter fused with 3′-UTR of Bcl-2 mRNA. HEK 293T cells were transfected with a pMIR-Bcl-2-3′-UTR or pMIR-Bcl-2-m3′-UTR. Meanwhile, the cells were cotransfected with an miR-15a/15b mimics or mimics NC. Compared with the mimics control, the 15a/15b mimics could reduce luciferase activity containing a wild-type miR-15a/15b binding site (**G** and **I**) but not a mutant binding site (**H** and **J**). $^{**}P<0.01$ vs mimics NC.

Bcl-2 by using the specific program TargetScan (Figure 3B). The data from Figure 3G and 3I show that miR-15a/15b may inhibit translation of Bcl-2 by directly acting on response elements specific for miR-15a/15b in the Bcl-2 3′-UTR region.

Knockdown of miR-15a/15b Regulates Luc-MSC Apoptosis Via Targeting VEGFR-2 and Bcl-2 In Vitro Experiment

To further explore the biological involvement of miR-15a/b in regulating luc-MSC apoptosis under OGD condition, miR-15a/15b expression was increased or blocked by its mimics or inhibitors. In our experiment, using the transfection method described in Materials and Methods section, we transfected the miR-15a/15b mimics or inhibitors into the luc-MSCs at 12 hours before OGD 12 hour treatment. As shown in Figure 4A and 4B, miR-15a/15b expression could be down-regulated with its inhibitors in vitro, which could be increased by its mimics treatment, as determined by qRT-PCR analysis. In addition, the results from Western blot showed that treatment of MSCs with miR-15a/15b inhibitors significantly increased VEGFR-2 and Bcl-2 expression level in luc-MSCs under the condition of OGD for 12 hours. However, treatment of luc-MSCs with miR-15a/15b mimics significantly decreased VEGFR2 (Figure 4C and 4D) and Bcl-2 (Figure 4E and 4F) expression level under the condition of OGD for 12 hours.

Next, the effect of miR-15a/15b on apoptosis in OGD-treated luc-MSCs using TUNEL analysis was investigated. Data from TUNEL assay showed that the percentage of apoptosis of each group was as follows: control, 6.3%±0.5%; OGD 12 hours; OGD 12 hours+miR-15a/15b inhibitors; and OGD 12 hours+miR-15a/15b mimics. From the above data,

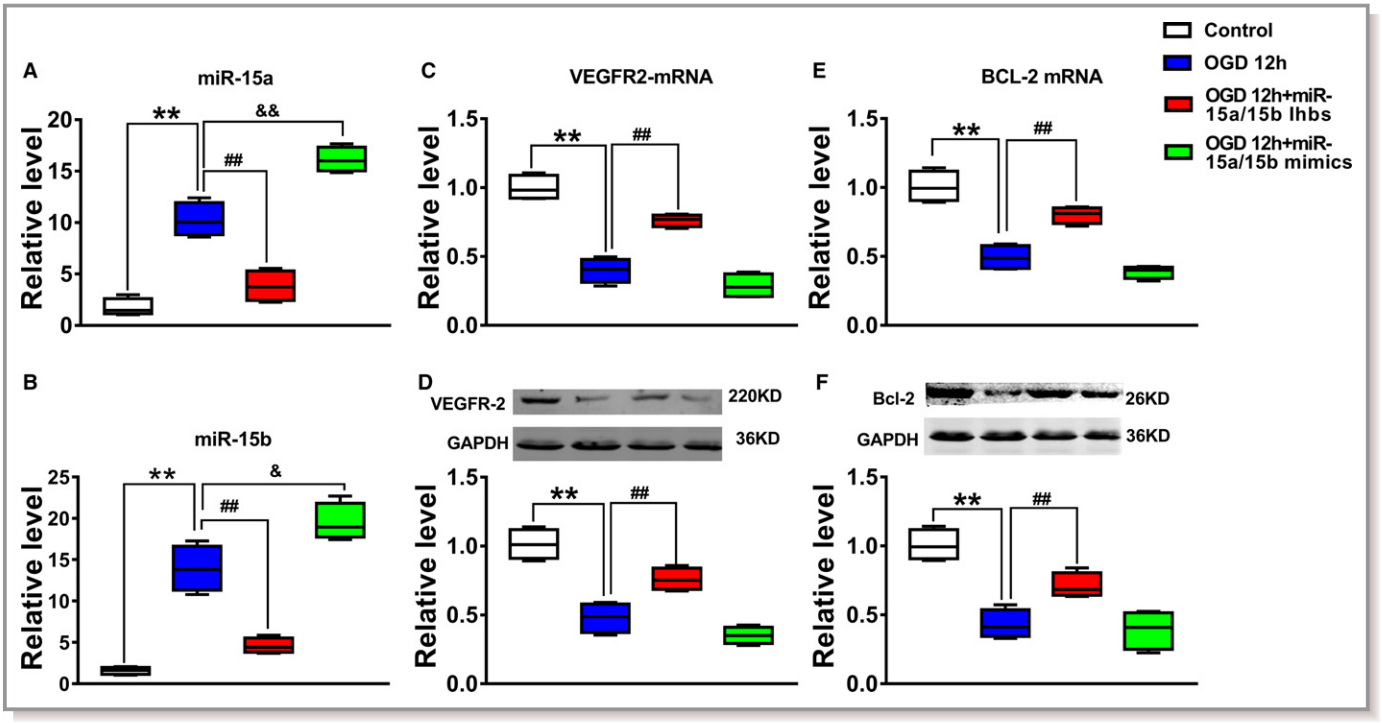

Figure 4. The effect of down-regulation of miR-15a/15b on apoptosis of mesenchymal stem cells under oxygen and glucose deprivation (OGD) condition. **A** and **B**, The expression levels of miR-15a and miR-15b from Control, OGD 12 hours, OGD 12 hours+miR-15a/15b inhibitors, and OGD 12 hours+miR-15a/15b mimics were detected by quantitative reverse transcription–polymerase chain reaction. Data are expressed as median (quartile 1–quartile 3), n=3. $^{**}P<0.01$ vs Control; $^{\#\#}P<0.01$ vs OGD 12 hour group; $^{\&}P<0.05$, $^{\&\&}P<0.01$ vs OGD 12 hour group. **C-F**, The expression levels of vascular endothelial growth factor receptor 2 (VEGFR2) (**C** and **D**) and Bcl-2 (**E** and **F**) from Control, OGD 12 hours, OGD 12 hours+miR-15a/15b inhibitors, and OGD 12 hours+miR-15a/15b mimics were detected by Western blotting assay. Data are expressed as median (quartile 1–quartile 3), n=3. $^{**}P<0.01$ vs Control; $^{\#\#}P<0.01$ vs OGD 12 hour group.

we concluded that down-regulation of miR-15a/15b markedly decreased luc-MSC apoptosis compared with control group ($P<0.05$) (Figure 5A and 5B), whereas overexpression of miR-15a/15b increased the apoptosis of luc-MSCs. Using fluorescein isothiocyanate–conjugated annexin V to label cell surface inverted phosphatidyl serine on apoptotic cells, we found that after pretreatment of miR-15a/15b inhibitors, the apoptotic rate of OGD-treated luc-MSCs decreased from 43.7±1.07% to 27.6±1.33%. However, treatment of OGD 12 hours and miR-15a/15b mimics did not markedly change the apoptotic rate of astrocytes induced by OGD treatment relative to OGD group (Figure 5C and 5D). Taken together, these results suggested that miR-15a/15b could act as an apoptosis inducer in luc-MSCs in vitro.

miR-15a/15b Modulates Luc-MSC Apoptosis Via Targeting VEGFR-2 and Its Downstream PI3K/Akt Signal Pathway

Previous study has experimentally disclosed that PI3K/Akt signal pathway was involved in regulating luc-MSC apoptosis. In this study, we first confirmed downregulation of miR-15a/15b played an antiapoptotic role via the regulation of VEGFR-2/PI3K/Akt signal pathway in luc-MSCs under OGD condition. The Western blotting results showed that treatment of MSCs with miR-15a/15b inhibitors significantly increased VEGFR-2 and its downstream proteins p-PI3K and p-AKT expression (Figure 6B and 6D), while it decreased Bax and caspase-3 expression (Figure 6E and 6F), demonstrating that miR-15a/15b inhibitors significantly inhibited luc-MSC apoptosis induced by OGD. However, the total PI3K and Akt expression was not influenced in all groups (Figure 6A and 6C). These data demonstrate that knockdown of miR-15a/15b improves the survival of MSCs via targeting VEGFR-2 and its downstream signal pathway. However, miR-15a/15b mimics treatment in MSCs could not obviously exert the same roles in antiapoptosis as miR-15a/15b inhibitors relative to OGD 12 hour group. So, the above results revealed that miR-15a/15b targeted VEGFR-2/PI3K/Akt signaling pathway and then inhibited apoptosis in MSCs under OGD condition.

Knockdown of miR-15a/15b Improves MSC Survival in Mouse MI Model Using BLI

To evaluate the effect of miR-15a/15b in regulating MSC survival after transplantation, we established mouse MI model

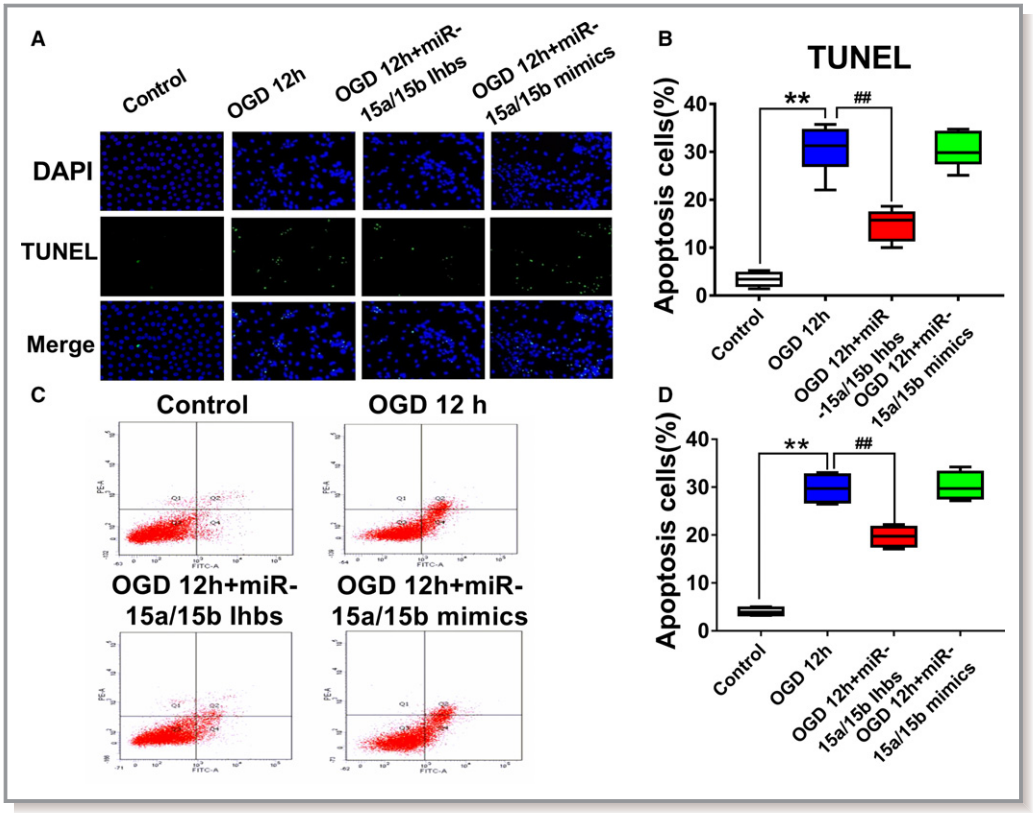

Figure 5. **A**, Apoptotic mesenchymal stem cells (MSCs) were determined by transferase-mediated deoxyuridine triphosphate–digoxigenin nick-end labeling (TUNEL) staining and visualized at ×200 magnification. Green color is TUNEL staining representing apoptotic cell; blue color is the cell nucleus stained by 4′,6-diamidino-2-phenylindole. **B**, The number of apoptotic cells was significantly increased in cells treated with oxygen and glucose deprivation (OGD) than in control group, whereas the downregulation of miR-15a/15b could attenuate the effect of OGD. Data are expressed as median (quartile 1–quartile 3), n=10. **C** and **D**, The apoptotic rate of luc-MSCs was detected by fluorescein isothiocyanate–annexin V labeling and flow cytometric analysis. Luc-MSCs were pretreated with miR-15a/15b inhibitors or with miR-15a/15b mimics under OGD 12 hours. miR-15a/15b inhibitors obviously inhibited the apoptotic rate of MSCs under OGD condition, whereas miR-15a/15b mimics could attenuate the proapoptotic role of OGD. The data are presented as the median (quartile 1–quartile 3) for 4 independent experiments. $^{**}P<0.01$ vs Control; $^{\#\#}P<0.01$ vs OGD group.

that thus allows us to directly visualize MSCs in infarcted myocardium using BLI in vivo (Figure 7A). To address this question, adult FVB/N mice were subjected to left anterior descending coronary artery ligation, followed by injection with 5×10^6 cultured luc-MSCs, luc-MSCs+miR-15a/15b inhibitors, or PBS. To assess MSC survival within the infarct zone, noninvasive imaging was performed on 1, 7, 14, 21, and 28 days (Figure 7B). Regions of interest were created over the precordium, and average radiance was measured. For the luc-MSC group, Fluc imaging signals were $3.54\pm0.25\times10^6$ photons/s/cm^2/sr on day 1, $3.06\pm0.21\times10^6$ photons/s/cm^2/sr on day 7, $2.59\pm0.10\times10^6$ photons/s/cm^2/sr on day 14, $1.16\pm0.13\times10^6$ photons/s/cm^2/sr on day 21, and $0.76\pm0.26\times10^6$ photons/s/cm^2/sr on day 28. For the luc-MSC+miR-15a/15b inhibitors group, Fluc imaging signals were $3.95\pm0.21\times10^6$ photons/s/cm^2/sr on day 1, $3.20\pm0.23\times10^3$ photons/s/cm^2/sr on day 7, $3.01\pm0.39\times10^3$ photons/s/cm^2/sr on day 14, $2.58\pm0.20\times10^3$ photons/s/cm^2/sr on day 21, and $1.85\pm0.98\times10^3$ photons/s/cm^2/sr on day 28. Background imaging signal (taken from regions of interest created on control nonrecipient animals given only D-luciferin) ranged between 1.0×10^5 and 6×10^6 photons/s/cm^2/sr. Quantitative analysis also showed that the luc-MSC+miR-15a/15b inhibitors group had significantly stronger chest Fluc activities at day 21 and day 28 compared with the luc-MSC group (Figure 7C). And ex vivo cardiac imaging results showed that peak bioluminescence signal of luc-MSC group was markedly lower than that of luc-MSC+miR-15a/15b inhibitors group (Figure 7D). In addition, fluorescence microscopy results also revealed clear evidence of Fluc$^+$ MSCs homing to the injured heart and further validated our BLI measurements in vivo and in vitro (Figure 7E).

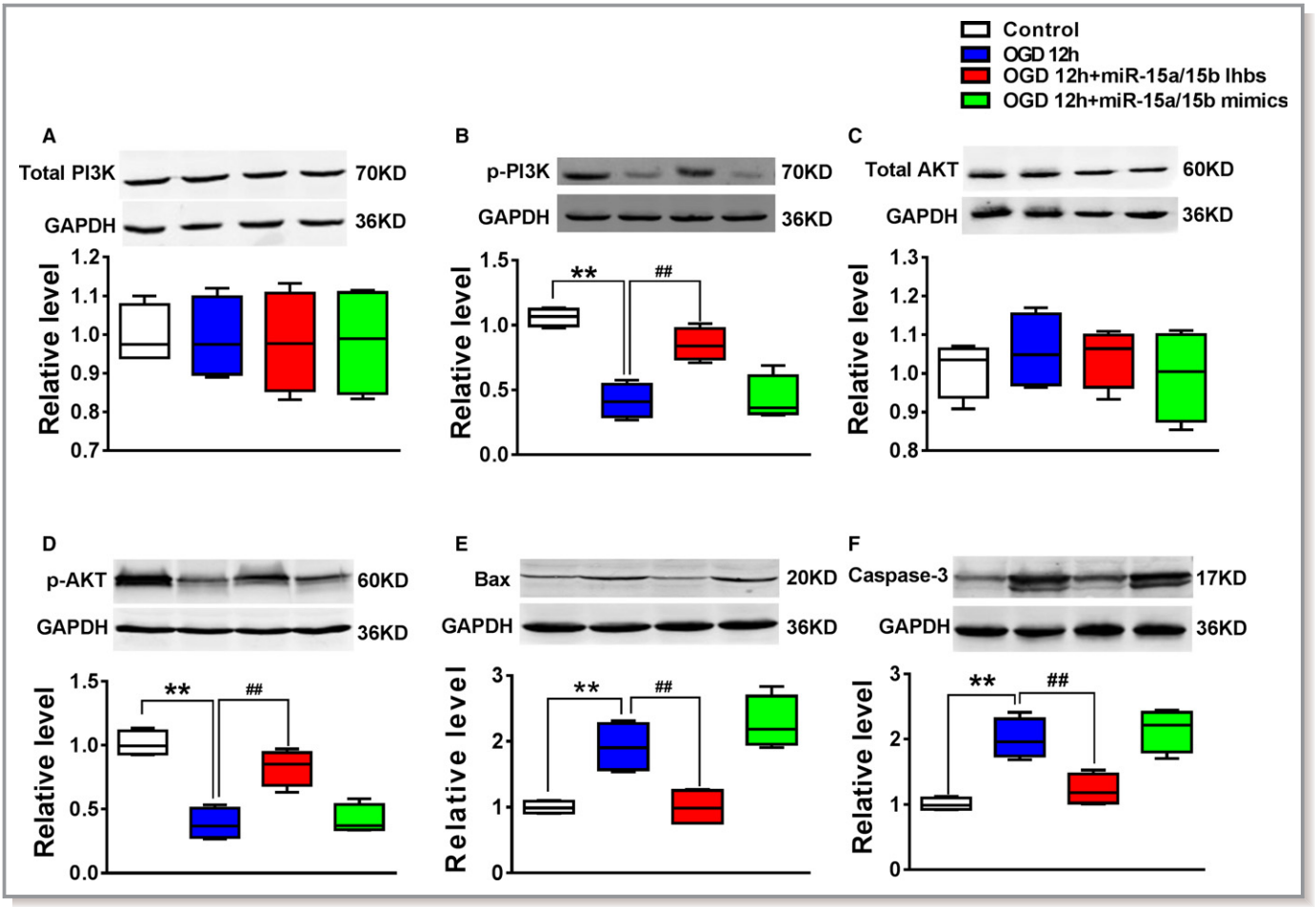

Figure 6. The expression levels of phosphatidylinositol 3-kinase (PI3K; **A**), p-PI3K (**B**), protein kinase B (AKT; **C**), p-AKT (**D**), Bax (**E**) and caspase-3 (**F**) from Control, OGD 12 hours, OGD 12 hours+miR-15a/15b inhibitors, and OGD 12 hours+miR-15a/15b mimics were detected by Western blotting assay. The data are presented as the median (quartile 1–quartile 3) for 4 independent experiments. $^{**}P<0.01$ vs Control; $^{\#\#}P<0.01$ vs oxygen and glucose deprivation (OGD) 12 hour group.

Functional Effects of Cell Transplantation

To determine whether intravenously delivered MSCs improved cardiac contractility, we performed echocardiography preoperatively and weekly postoperatively. Representative M-mode images of mice injected with PBS, luc-MSCs, or luc-MSCs+miR-15a/15b inhibitors at week 4 are shown in Figure 8. By 4 weeks, echocardiographic examination showed that, relative to PBS group, the fractional shortening and ejection fraction of luc-MSC group were increased, whereas the left ventricular end-diastolic diameter and left ventricular end-systolic diameter were decreased, but left ventricular end-systolic diameter decrease did not reach statistical significance (Figure 8C through 8F). Moreover, the ejection fraction and fractional shortening in the luc-MSC+miR-15a/15b inhibitors group were increased markedly compared with luc-MSC group, whereas the left ventricular end-diastolic dimensions and left ventricular end-systolic dimensions were further decreased in the luc-MSC+miR-15a/15b inhibitors group (Figure 8C through 8F). Accordingly, the data from Figure 8G further showed that MI-induced cardiac fibrosis could be partially reversed by MSC transplantation, especially in the luc-MSC+miR-15a/15b inhibitors group. These data indicated that luc-MSC transplantation can improve the MI heart function in vivo and miR-15a/15b is involved in modulating survival of MSCs to further improve their therapeutic efficacy of MI.

Discussion

The MSCs were the most commonly used cell types for treating patients with MI in clinical trials because of their multipotent differentiation potential and proangiogenic as well as immunomodulatory properties. However, one of the main obstacles for successful stem cell–based regeneration and repair for cardiac regeneration after myocardial injury remains unmet challenges largely attributable to low viability of cells transplanted in the recipient sites, which remarkably compromises therapeutic efficacy and outcomes. Growing

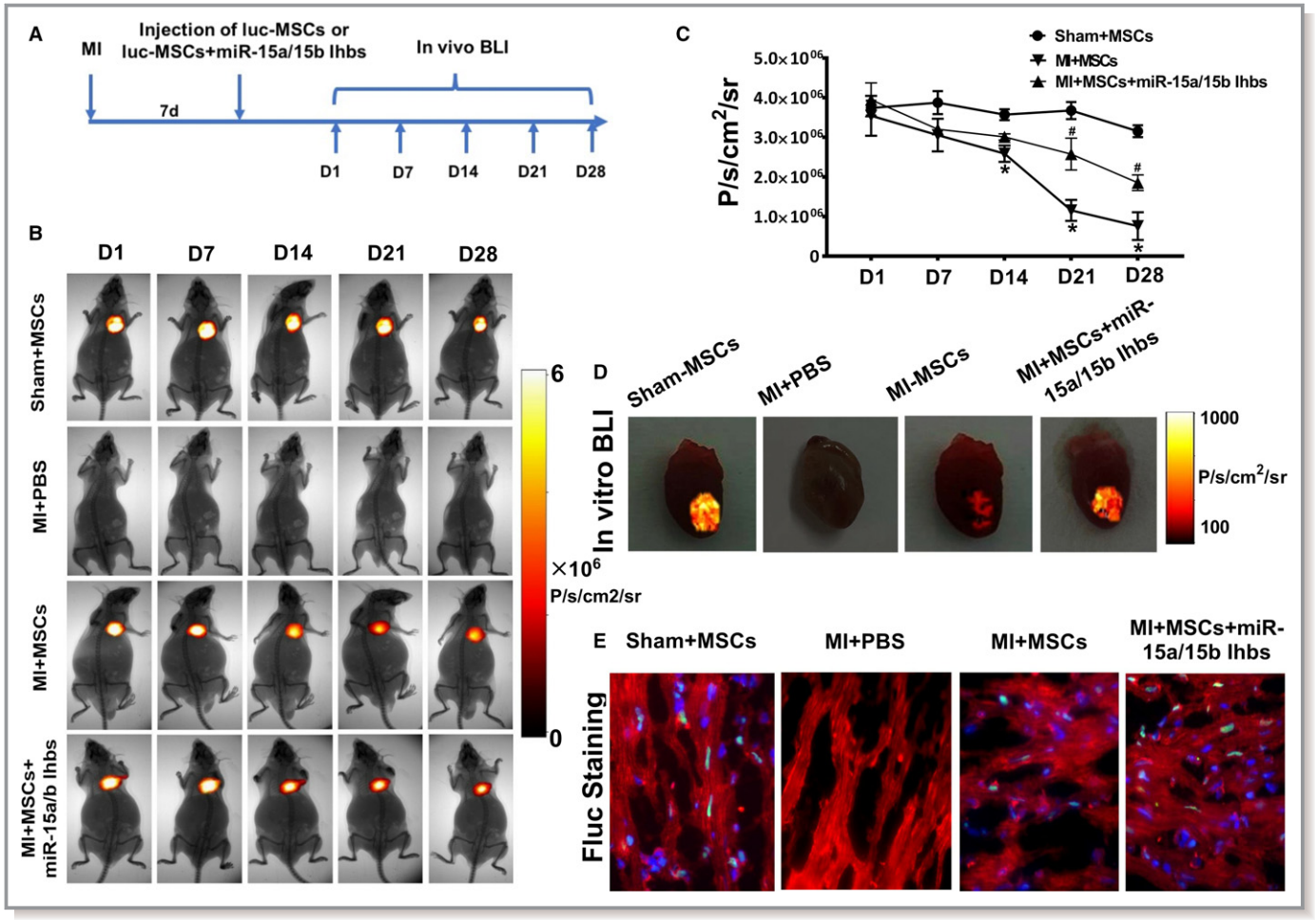

Figure 7. In vivo visualization and region of interest (ROI) analysis of firefly luciferase gene (Fluc) activities to monitor the mesenchymal stem cells (MSCs) in the animal model. **A**, Schematic diagram of experimental process in vivo. **B**, Bioluminescence imaging (BLI) of luc-MSCs in PBS, luc-MSC, and luc-MSC+miR-15a/15b inhibitors groups in myocardial infarction (MI) animal models. Color scale bar values are in photons per square centimeter per second per steradian (P/s/cm^2/sr). **C**, Quantitative signals from imaging in vivo were obtained by ROI analysis and were shown next to the mouse picture. The BLI results showed a drastic decrease in Fluc activities of luc-MSCs in the MI group after 14 days in vivo, and the quantitative imaging signals from luc-MSC group nearly reduced by half. However, the reduction of imaging signals could be reversed by coapplication of miR-15a/15b inhibitors. Data are expressed as median (quartile 1–quartile 3), n=5 independent experiments for each condition. **D**, BLI of luc-MSCs in Sham+MSC, MI+PBS, MI+MSC, and luc-MSC+miR-15a/15b inhibitors hearts in vitro. Color scale bar values are in P/s/cm^2/sr. **E**, Fluorescence microscopy of Fluc$^+$ MSCs in hearts from luc-MSC and luc-MSC+miR-15a/15b inhibitors groups, but no Fluc$^+$ staining in heart tissues from MI+PBS group. $^*P<0.05$ vs luc-MSC group. $^{\#}P<0.05$ vs MI+MSCs group.

evidence has shown that microRNAs are involved in regulating the survival and effects of stem cells in vitro and in vivo, and they light a new way for us to study the potential of microRNAs as diagnostic markers and therapeutic targets in stem cell transplantation for cardiovascular diseases.[14,24,25] Cai et al have manifested that cross talk between MSCs and cardiomyocytes contributes to mitigate myocardial hypertrophy via inhibiting Ca^{2+}/calcineurin/Nuclear factor of activated T cells C3 (NFATc3) hypertrophic pathways in cardiomyocytes.[26] Recently, Ham et al have elucidated that microRNA-modified MSCs were more effective and conducive to repair of infarct injury and improved heart function by enhancing transplanted cell survival and cardiomyogenic differentiation, thus highlighting the benefits and potential of microRNA-modified MSCs in the treatment of ischemic heart disease.[27] Our current study documented that down-regulation of miR-15a/15b may play an obvious role in improving survival of MSCs under OGD condition or in the harsh microenvironment in infarcted heart.

It is well known that acutely or chronically injured myocardium represents harsh environment not only for its own cardiomyocytes but also for the transplanted cells. And serious myocardial ischemia may lead to the permanent loss of cardiomyocytes and subsequent left ventricular pathological alterations that ultimately lead to heart failure. Although lower survival of cell transplants in the damaged tissue is also well known and has been described before, there are 2 main aspects that should be attributed to the problem of poor

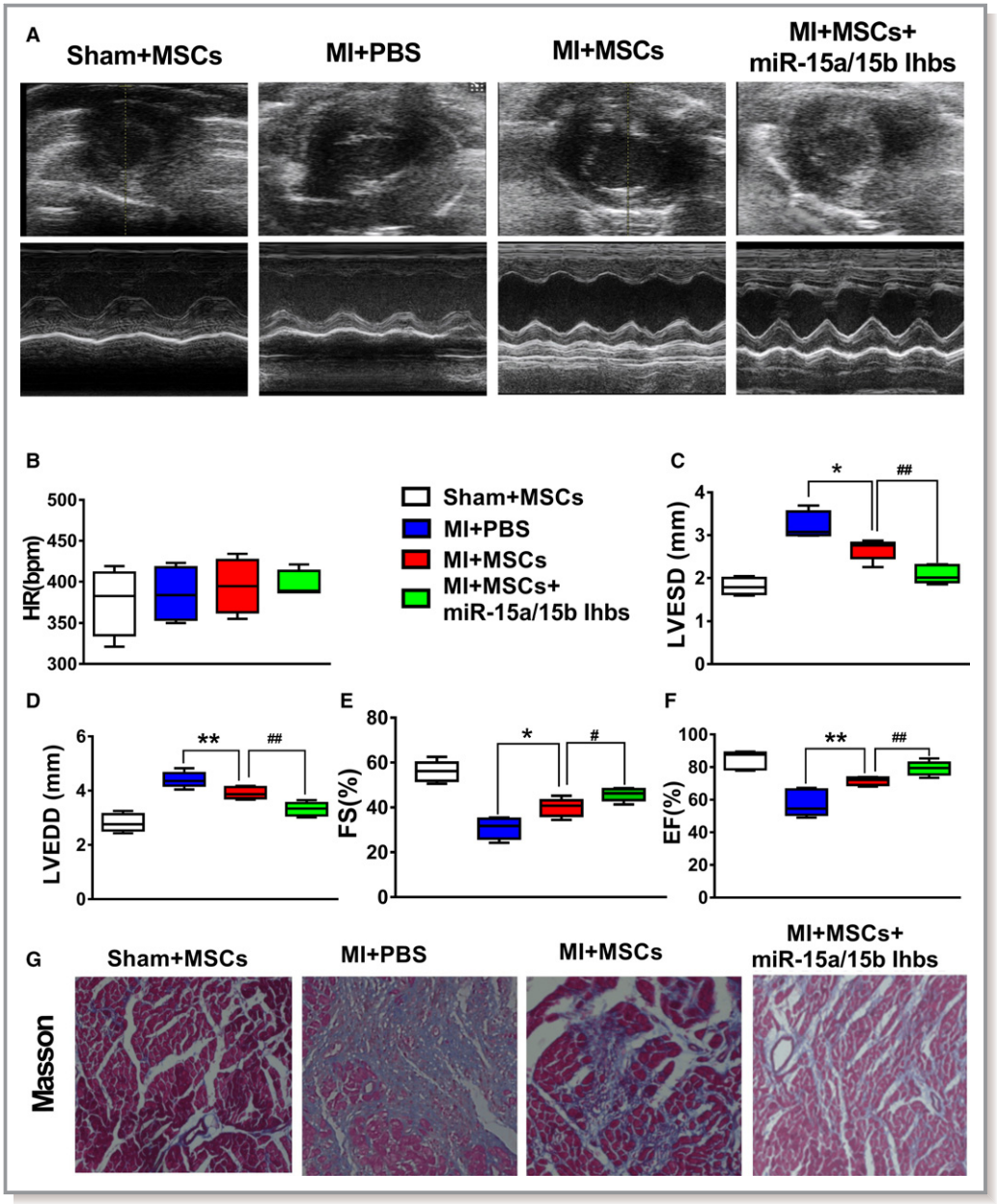

Figure 8. Effects of cell transplantation on heart function. **A**, Representative M-mode echocardiographs from PBS, luc-mesenchymal stem cells (MSCs), and luc-MSCs+miR-15a/b inhibitors. **B** through **F**, Heart rate (beats per minute [bpm]), left ventricular end-systolic diameter (LVESD), left ventricular end-diastolic diameter (LVEDD), fractional shortening (FS), and ejection fraction (EF) from PBS, luc-MSC, and luc-MSC+miR-15a/b inhibitors groups. Data are expressed as median (quartile 1–quartile 3), n=5 independent experiments for each condition. **G**, Masson trichrome staining from mice with myocardial infarction (MI) treated with PBS, luc-MSCs, and luc-MSCs+miR-15a/b inhibitors. The collagen was stained blue. $^{*}P<0.05$, $^{**}P<0.01$ vs PBS group; $^{\#}P<0.05$ vs luc-MSC group; $^{\#\#}P<0.01$ vs luc-MSC group.

viability of transplanted cells during therapy. The first one is that transplantable cells may be not prepared to withstand such harsh environment. The second issue is that damaged tissue becomes repellent (ie, acidic, hypoxic, glucose deprived, and under inflammation). So, enduring the prodeath environment in the ischemic myocardial tissue is an obstacle that represents a great challenge for patient recovery and for clinical trials using stem cell treatment. To mimics the harsh myocardial ischemic environment in vivo, we cultured the luc-MSCs under OGD condition in vitro. The MSC viability determined by MTT analysis was reduced nearly by 35% in cells on OGD for 12 hours. Next, we investigated the possible cytoprotective effect of miR-15a/15b on OGD-induced damage in MSCs. The cells were pretreated with miR-15a/15b

inhibitors or mimics and then cultured under OGD condition for 12 hours. The results from the current study showed that pretreatment with miR-15a/15b inhibitors exerted a remarkable cytoprotective effect, which could effectively reduce OGD-induced cell death of MSCs, whereas the miR-15a/15b mimics did not have the same roles.

PI3K/Akt pathway is well known to be a major cell survival pathway, and the activation of the PI3K/Akt pathway enhances resistance to cell apoptosis. Studies of major molecular survival pathways showed great potential for applying PI3K/AKT signaling pathway in providing stem cell protection. This can be exemplified by the findings that overexpression of AKT can block apoptotic cell death of MSCs and thus improve cardiac function.[28] Using microRNA target predictions (TargetScan, http://www.targetscan.org), we found that VEGFR-2 is the potential target of miR-15a/15b. However, until now, the definite cytoprotective effect of miR-15a/15b on MSCs under OGD condition has not been clarified in detail. In accord with previous study, our data also disclosed that knockdown of miR-15a/15b levels was able to inhibit OGD-induced MSC apoptosis via targeting VEGFR-2 and downstream PI3K/AKT signaling pathway. In addition, Bcl-2 is another potential target of miR-15a/15b; knockdown of miR-15a/15b levels via its inhibitors may directly target Bcl-2 and increase its expression level in MSCs, which partly plays the antiapoptotic effects in MSCs under OGD condition. Moreover, the TUNEL and fluorescence-activated cell sorting results in our current study also documented that knockdown of miR-15a/15b in MSCs could inhibit OGD-induced MSC apoptosis.

However, the success of MSC therapy will likely require novel methods to disclose the long-term fate of transplanted cells and dynamic biodistribution without reliance on postmortem histological features. In recent years, several molecular imaging techniques have been developed to better understand stem cell fate in vitro and in vivo.[29–31] Recently, labeling MSCs with reporter gene genetically and the use of corresponding imaging modality provide a novel, noninvasive method for serially tracking and quantifying the fate of administered MSCs in vivo.[32] In the current study, bone marrow MSCs were isolated from the luciferase transgenic FVB mice, which provided the opportunity to obtain a clear understanding of implanted cell fate via BLI technique. The results of the in vitro BLI analysis from this study demonstrated that, compared with no OGD stimulation, the Fluc activity of luc-MSCs decreased gradually with prolongation of OGD stimulation, especially at 12 and 24 hours OGD treatment. And the percentage bioluminescence signals from miR-15a/15b inhibitors treatment group markedly increased relative to OGD treatment group. In the same way, knockdown of miR-15a/15b improves luc-MSC survival in mouse MI model using BLI analysis in vivo and in vitro. In the ischemic heart failure trials, studies have already started to show improvements in regional and global systolic and diastolic function, reversal of left ventricular remodeling, decrease of fibrosis deposition, and enhanced myocardial collateralization using the regenerative potential of MSCs.[33,34] In our current study, we also found that knockdown of miR-15a/15b in MSCs could reverse the mice heart function and fibrosis deposition within MI zone.

Taken together, in this study, we disclosed the important role of specific microRNAs in the control of MSC survival and pointed out that miR-15a/15b could be used as potential intervention targets for the treatment of cardiac MSCs. Regulating microRNA expression in stem cells is likely to emerge as an alternative and safe method to treat ischemic heart disease. However, our current research was performed in mouse models and the findings could not be extrapolated directly to humans. Additional studies are required to investigate whether the miR-15a/15b mechanism in stem cells also operates in the clinical setting.

Conclusion

Overall, the results of the present study provide preliminary evidence indicating that knockdown of miR-15a/15b has beneficial effects on MSCs by promoting proliferation, inhibiting apoptosis, increasing VEGFR-2 expression, and improving its survival within MI zone. In addition, the beneficial effects of miR-15a/15b are possibly a result of the activation of the VEGFR-2/PI3K/AKT signaling pathway. Furthermore, BLI strategy provides a unique and powerful method to monitor the stem cells in vitro and in vivo, which will be extremely valuable in the diagnosis and treatment application of clinical patients in the future. These data collectively demonstrate that miR-15a/15b may be considered a candidate for optimizing MSC-based cell therapy.

Author Contributions

Tu: conception and design, collection and assembly of data, data analysis and interpretation; Qiu: collection and assembly of data; L. Liu: collection and assembly of data; Y.B. Liu: collection of data; Tang: provision of study material; Fan: data analysis and interpretation, manuscript writing; Yu: conception and design, financial support, manuscript writing, and final editing of manuscript.

Sources of Funding

This work was supported, in part, by the National Natural Science Foundation of China (81871402, 81671746, 81401457, 81503069, 81330033, and 81601150), National Key R&D Program of China (2016YFC1301100), the China Postdoctoral

Science Foundation (2015M571449, 2015M581490, and 2014M561376), and the Special Financial Grant from China Postdoctoral Science Foundation (2016T90313 and 2016T90316).

Disclosures

None.

References

1. Morys JM, Bellwon J, Hofer S, Rynkiewicz A, Gruchala M. Quality of life in patients with coronary heart disease after myocardial infarction and with ischemic heart failure. *Arch Med Sci*. 2016;12:326–333.
2. Quinones A, Lobach I, Maduro GA Jr, Smilowitz NR, Reynolds HR. Diabetes and ischemic heart disease death in people age 25-54: a multiple-cause-of-death analysis based on over 400 000 deaths from 1990 to 2008 in New York City. *Clin Cardiol*. 2015;38:114–120.
3. Yin L, Huang D, Liu X, Wang Y, Liu J, Liu F, Yu B. Omentin-1 effects on mesenchymal stem cells: proliferation, apoptosis, and angiogenesis in vitro. *Stem Cell Res Ther*. 2017;8:224.
4. Lee CY, Kim R, Ham O, Lee J, Kim P, Lee S, Oh S, Lee H, Lee M, Kim J, Chang W. Therapeutic potential of stem cells strategy for cardiovascular diseases. *Stem Cells Int*. 2016;2016:4285938.
5. Klopsch C, Skorska A, Ludwig M, Gaebel R, Lemcke H, Kleiner G, Beyer M, Vollmar B, David R, Steinhoff G. Cardiac mesenchymal stem cells proliferate early in the ischemic heart. *Eur Surg Res*. 2017;58:341–353.
6. Li JY, Ke HH, He Y, Wen LN, Xu WY, Wu ZF, Zhao YM, Zhong GQ. Transplantation of mesenchymal stem cells modulated Cx43 and Cx45 expression in rats with myocardial infarction. *Cytotechnology*. 2018;70:225–234.
7. Zhang F, Wang C, Lin J, Wang X. Oxidized low-density lipoprotein (ox-LDL) promotes cardiac differentiation of bone marrow mesenchymal stem cells via activating ERK1/2 signaling. *Cardiovasc Ther*. 2017;35:e12305.
8. El Sayed Shafei A, Ali MA, Ghanem HG, Shehata AI, Abdelgawad AA, Handal HR, Talaat KA, Ashaal AE, El-Shal AS. Mesenchymal stem cell therapy: a promising cell based therapy for treatment of myocardial infraction. *J Gene Med*. 2017;19.
9. Abdelwahid E, Kalvelyte A, Stulpinas A, de Carvalho KA, Guarita-Souza LC, Foldes G. Stem cell death and survival in heart regeneration and repair. *Apoptosis*. 2016;21:252–268.
10. RajendranNair DS, Karunakaran J, Nair RR. Differential response of human cardiac stem cells and bone marrow mesenchymal stem cells to hypoxia-reoxygenation injury. *Mol Cell Biochem*. 2017;425:139–153.
11. Saraswati S, Guo Y, Atkinson J, Young PP. Prolonged hypoxia induces monocarboxylate transporter-4 expression in mesenchymal stem cells resulting in a secretome that is deleterious to cardiovascular repair. *Stem Cells*. 2015;33:1333–1344.
12. Chendrimada TP, Finn KJ, Ji X, Baillat D, Gregory RI, Liebhaber SA, Pasquinelli AE, Shiekhattar R. MicroRNA silencing through RISC recruitment of EIF6. *Nature*. 2007;447:823–828.
13. Gnecchi M, Pisano F, Bariani R. MicroRNA and cardiac regeneration. *Adv Exp Med Biol*. 2015;887:119–141.
14. White MC, Pang L, Yang X. MicroRNA-mediated maturation of human pluripotent stem cell-derived cardiomyocytes: towards a better model for cardiotoxicity? *Food Chem Toxicol*. 2016;98:17–24.
15. Zhu K, Liu D, Lai H, Li J, Wang C. Developing miRNA therapeutics for cardiac repair in ischemic heart disease. *J Thorac Dis*. 2016;8:E918–E927.
16. Seo HH, Lee SY, Lee CY, Kim R, Kim P, Oh S, Lee H, Lee MY, Kim J, Kim LK, Hwang KC, Chang W. Exogenous miRNA-146a enhances the therapeutic efficacy of human mesenchymal stem cells by increasing vascular endothelial growth factor secretion in the ischemia/reperfusion-injured heart. *J Vasc Res*. 2017;54:100–108.
17. Lee SY, Ham O, Cha MJ, Song BW, Choi E, Kim IK, Chang W, Lim S, Lee CY, Park JH, Lee J, Bae Y, Seo HH, Choi E, Jang Y, Hwang KC. The promotion of cardiogenic differentiation of hMSCs by targeting epidermal growth factor receptor using microRNA-133a. *Biomaterials*. 2013;34:92–99.
18. Tu Y, Liu L, Zhao D, Liu Y, Ma X, Fan Y, Wan L, Huang T, Cheng Z, Shen B. Overexpression of miRNA-497 inhibits tumor angiogenesis by targeting VEGFR2. *Sci Rep*. 2015;5:13827.
19. Liu Q, Fu H, Sun F, Zhang H, Tie Y, Zhu J, Xing R, Sun Z, Zheng X. miR-16 family induces cell cycle arrest by regulating multiple cell cycle genes. *Nucleic Acids Res*. 2008;36:5391–5404.
20. Liu JL, Jiang L, Lin QX, Deng CY, Mai LP, Zhu JN, Li XH, Yu XY, Lin SG, Shan ZX. MicroRNA 16 enhances differentiation of human bone marrow mesenchymal stem cells in a cardiac niche toward myogenic phenotypes in vitro. *Life Sci*. 2012;90:1020–1026.
21. Huang S, Xu L, Sun Y, Zhang Y, Li G. The fate of systemically administrated allogeneic mesenchymal stem cells in mouse femoral fracture healing. *Stem Cell Res Ther*. 2015;6:206.
22. Liu L, You Q, Tu Y, Li Q, Zheng L, Li X, Gu J, Wang G. Midazolam inhibits the apoptosis of astrocytes induced by oxygen glucose deprivation via targeting JAK2-STAT3 signaling pathway. *Cell Physiol Biochem*. 2015;35:126–136.
23. Tu Y, Wan L, Zhao D, Bu L, Dong D, Yin Z, Cheng Z, Shen B. In vitro and in vivo direct monitoring of miRNA-22 expression in isoproterenol-induced cardiac hypertrophy by bioluminescence imaging. *Eur J Nucl Med Mol Imaging*. 2014;41:972–984.
24. Song YS, Joo HW, Park IH, Shen GY, Lee Y, Shin JH, Kim H, Kim KS. Bone marrow mesenchymal stem cell-derived vascular endothelial growth factor attenuates cardiac apoptosis via regulation of cardiac miRNA-23a and miRNA-92a in a rat model of myocardial infarction. *PLoS One*. 2017;12:e0179972.
25. Shen X, Pan B, Zhou H, Liu L, Lv T, Zhu J, Huang X, Tian J. Differentiation of mesenchymal stem cells into cardiomyocytes is regulated by miRNA-1-2 via WNT signaling pathway. *J Biomed Sci*. 2017;24:29.
26. Cai B, Tan X, Zhang Y, Li X, Wang X, Zhu J, Wang Y, Yang F, Wang B, Liu Y, Xu C, Pan Z, Wang N, Yang B, Lu Y. Mesenchymal stem cells and cardiomyocytes interplay to prevent myocardial hypertrophy. *Stem Cells Transl Med*. 2015;4:1425–1435.
27. Ham O, Lee SY, Lee CY, Park JH, Lee J, Seo HH, Cha MJ, Choi E, Kim S, Hwang KC. Let-7b suppresses apoptosis and autophagy of human mesenchymal stem cells transplanted into ischemia/reperfusion injured heart 7by targeting caspase-3. *Stem Cell Res Ther*. 2015;6:147.
28. Mangi AA, Noiseux N, Kong D, He H, Rezvani M, Ingwall JS, Dzau VJ. Mesenchymal stem cells modified with Akt prevent remodeling and restore performance of infarcted hearts. *Nat Med*. 2003;9:1195–1201.
29. Sheikh AY, Lin SA, Cao F, Cao Y, van der Bogt KE, Chu P, Chang CP, Contag CH, Robbins RC, Wu JC. Molecular imaging of bone marrow mononuclear cell homing and engraftment in ischemic myocardium. *Stem Cells*. 2007;25:2677–2684.
30. van der Bogt KE, Hellingman AA, Lijkwan MA, Bos EJ, de Vries MR, van Rappard JR, Fischbein MP, Quax PH, Robbins RC, Hamming JF, Wu JC. Molecular imaging of bone marrow mononuclear cell survival and homing in murine peripheral artery disease. *JACC Cardiovasc Imaging*. 2012;5:46–55.
31. Zhang WY, Ebert AD, Narula J, Wu JC. Imaging cardiac stem cell therapy: translations to human clinical studies. *J Cardiovasc Transl Res*. 2011;4:514–522.
32. Li SH, Lai TY, Sun Z, Han M, Moriyama E, Wilson B, Fazel S, Weisel RD, Yau T, Wu JC, Li RK. Tracking cardiac engraftment and distribution of implanted bone marrow cells: comparing intra-aortic, intravenous, and intramyocardial delivery. *J Thorac Cardiovasc Surg*. 2009;137:1225–1233.e1221.
33. Silva GV, Litovsky S, Assad JA, Sousa AL, Martin BJ, Vela D, Coulter SC, Lin J, Ober J, Vaughn WK, Branco RV, Oliveira EM, He R, Geng YJ, Willerson JT, Perin EC. Mesenchymal stem cells differentiate into an endothelial phenotype, enhance vascular density, and improve heart function in a canine chronic ischemia model. *Circulation*. 2005;111:150–156.
34. Mathiasen AB, Qayyum AA, Jorgensen E, Helqvist S, Fischer-Nielsen A, Kofoed KF, Haack-Sorensen M, Ekblond A, Kastrup J. Bone marrow-derived mesenchymal stromal cell treatment in patients with severe ischaemic heart failure: a randomized placebo-controlled trial (MSC-HF trial). *Eur Heart J*. 2015;36:1744–1753.